Biochimica et Biophysica Acta, 1059 (1991) 181–188

ADONIS 0005272891001958

BBABIO 43450

Identification and characterisation of EPR signals involving Q_B semiquinone in plant Photosystem II

Beverly J. Hallahan, Stuart V. Ruffle, Simon J. Bowden and Jonathan H.A. Nugent

Department of Biology, University College London, London (U.K.)

(Received 12 December 1990)

Key words: EPR; Photosystem II; Iron-quinone; Reaction center; Halogenated 1,4-benzoquinone; Semiquinone; (Plant)

We have investigated the EPR characteristics of native Q_B and Q_B analogues in higher plant PS II. We show that, as in cyanobacteria, an interaction between Q_A and Q_B iron-semiquinones (Q_A^--Fe^{2+}-Q_B^-) is observed which gives an EPR signal near $g = 1.6$. Bicarbonate binding close to the non-haem iron is required to observe this interaction. The EPR signal of Q_B semiquinone is weak and difficult to distinguish from that of Q_A. The appearance of the $g = 1.6$ signal from Q_A^--Fe^{2+}-Q_B^- after 77 K illumination is a better marker for the presence of Q_B semiquinone. The yield of Q_B semiquinone in plant PS II is lower than found in cyanobacteria. The brominated quinones DBMIB, TBTQ and bromanil were used as Q_B analogues to increase the yield of Q_A^--Fe^{2+}-Q_B^-. These analogues act by forming a stable semiquinone at the Q_B site and not by covalent binding.

Introduction

Photosystem II (PS II) of cyanobacteria, algae and higher plants is a membrane-protein complex which catalyses the light-induced transfer of electrons from water to plastoquinone. The reaction centre core shows homology with that of the more highly characterised reaction centre of purple photosynthetic bacteria [1,2].

In purple bacteria, the quinone electron acceptors Q_A and Q_B bind to the reaction centre polypeptides L and M. Similar binding sites for Q_A and Q_B of PS II have been proposed involving the polypeptides D1 (Q_B) and D2 (Q_A), which show homology to the L and M polypeptides [1]. In both PS II and purple bacteria, a non-haem iron atom is located between the two quinone binding sites [1,2].

Q_A is a single electron carrier, whereas a two-step plastoquinone reduction and protonation occur at the Q_B site. The plastoquinone binds to the Q_B site and accepts an electron from Q_A^- forming the tightly bound semiquinone [3,4]. Following another turnover of the reaction centre, a second electron is transferred from Q_A^-. After protonation, the plastoquinol formed has low binding affinity and is released or exchanged with plastoquinone. In PS II, the non-haem iron can be oxidised by ferricyanide and by some exogenous quinones which act through the Q_B site [5,6]. The Q_B binding niche is also the site of interaction of some types of electron transport inhibitor. These include the phenolic and urea type of herbicide inhibitor as well as substituted benzoquinones [7].

The semiquinones of Q_A and Q_B, produced either chemically or photochemically, can be detected by EPR. The lineshape and g-value of the signal obtained is influenced by the nearby non-haem iron and the resulting 'iron-semiquinone' spectrum of both Q_A^- and Q_B^- are broad. In purple bacteria, both Q_A^--Fe^{2+} and Q_B^--Fe^{2+} give similar EPR signals with first derivative peaks near $g = 1.8$ [8].

In PS II the situation is complex, with more than one lineshape form of Q_A^--Fe^{2+} occurring. Initially, a signal with a lineshape similar to that of purple bacteria was identified (the $g = 1.8$ signal) [9,10]. Subse-

Abbreviations: DBMIB, 2,5-dibromo-3-methyl-6-isopropyl 1,4-benzoquinone; TBTQ, (Tribromotoluquinone), 2,3,5-tribromo-6-methyl 1,4-benzoquinone; Bromanil, 2,3,5,6-tetrabromo-1,4-benzoquinone; PPBQ, phenyl-1,4-benzoquinone; DCBQ, 2,5-dichloro-1,4-benzoquinone; DCMU, 3-(3,4-dichlorophenyl)-1,1-dimethylurea; Hepes, *N*-2-hydroxyethylpiperazine-*N'*-2-ethanesulfonic acid; Mes, 2(*N*-morpholino)ethanesulfonic acid; HTG, *n*-heptyl thioglucoside; EPR, electron paramagnetic resonance spectrometry; OP, 1,10-phenanthroline; FCCP, carbonyl cyanide *p*-(trifluoromethoxy)phenylhydrazone.

Correspondence: J. Nugent, Department of Biology, Darwin Building, University College London, Gower Street, London, WC1E 6BT, U.K.

quently two more signals were identified, the $g = 1.9$ signal [11] and the $g = 1.6$ signal [12,13]. The $g = 1.9$ and $g = 1.8$ signals were observed under different conditions, the $g = 1.9$ signal being seen above pH 7 and when bicarbonate was bound to the PS II reaction centre and the $g = 1.8$ signal at low pH and when bicarbonate was displaced by formate [14]. In the purple bacterial reaction centre the ligands to the non-haem iron are four histidines and a glutamate [1,2]. In PS II, the bicarbonate has been suggested to bind to the non-haem iron replacing one or both of the glutamate ligands found in purple bacteria (Refs. 1,13,15–18 and Nugent and co-workers, unpublished data).

The $g = 1.6$ iron-semiquinone signal was found in cyanobacterial PS II preparations [12,13] and identified as arising from either the interaction of Q_A and Q_B iron-semiquinones in the same centre [13] or from a different conformational form of Q_A^--Fe^{2+} resulting from structural differences between cyanobacterial and plant binding sites [12]. We have recently shown that the signal is indeed formed by the interaction of Q_A and Q_B iron-semiquinones [20].

The EPR spectrum of Q_B^--Fe^{2+} in PS II has received less attention. Rutherford et al. have suggested that a $g = 1.9$ form occurs [21], whilst a $g = 1.8$ form and $g = 1.9$ signal have also been attributed to Q_B^--Fe^{2+} [22].

We have now characterised EPR signals from the native Q_B semiquinone and halogenated Q_B analogues in higher plant PS II. We show that an interaction between the Q_A and Q_B semiquinones occurs, as in cyanobacteria. This requires the bicarbonate-bound form of PS II, accounting for the lack of this signal in purple bacteria. Our results also allow further explanation of the effects of brominated 1,4-benzoquinones on PS II [23–26]. The understanding of the conditions required for each iron-semiquinone lineshape now enables preparations with characteristic spectra to be defined.

Materials and Methods

Chloroplast thylakoid membranes (12 mg Chl/ml) and PS-II-enriched membranes were prepared by the method of Ford and Evans [27] from market spinach (*Spinacea oleracea*), barley mutant zb^{63} (*Hordeum vulgare*) or pea (*Pisum sativum*) var. Feltham First. A Triton X-100 detergent/Chl ratio of 22.5/1 was used at an incubation concentration of 2 mg Chl/ml. Samples were stored and used in 20 mM Mes-NaOH, 5 mM $MgCl_2$, 15 mM NaCl and 20% (v/v) glycerol (pH 6.3). For samples at pH 7.5, a buffer of 40 mM Hepes, 10 mM NaCl, 5 mM $MgCl_2$, 20% glycerol (pH 7.5) was used. Pea or spinach PS II membranes (BBY's 10 mg Chl/ml)) showed identical characteristics for these experiments.

HTG PS II (4–5 mg Chl/ml) was prepared by a method based on that of Enami et al. [28] described in Ref. 29. Chl *a* and *b* measurements were made using the method in Ref. 30. EPR was used to check batches of BBY's to ensure that samples initially contained centres with bicarbonate bound (i.e., no $g = 1.8$ type Q_A iron semiquinone signal). PS II preparations were also checked to ensure that PS I and the cytochrome b_6/f complex were absent, so that any effects were clearly attributable to PS II.

PS II (1 mg Chl/ml) from the cyanobacterium *Phormidium laminosum* was prepared as in Ref. 13 based on the method of Stewart and Bendall [31] but using the detergent *N*-dodecyl-*N*,*N*-dimethylammonio-3-propanesulfonate (Serva, Heidelberg) [32]. It was resuspended in 10 mM Hepes 10 mM $MgCl_2$, 5 mM disodium hydrogen phosphate and 25% v/v glycerol (pH 7.5).

Duplicate 0.3 ml samples in 3 mm diameter EPR tubes were treated as described in the figure legends. Dimethylsulfoxide or ethanol used as solvent for quinones and herbicides was kept below 2% (v/v). Quinones (DCBQ, PPBQ TBTQ, DBMIB and bromanil) were used at a concentration of 500 μM, DCMU at 200 μM, OP at 1 mM and FCCP at 250 μM.

PS II samples were illuminated for 30 s at room temperature with a 650 W light source fitted with a 2.5 cm water heat filter. They were then dark adapted for 30–45 min. These conditions were found to maximise Q_B semiquinone levels [20] and termed the 'Q_B semiquinone protocol'. The samples were then frozen to 77 K and stored at 77 K in darkness until EPR spectra were taken.

77 K illumination of PS II to reduce Q_A was performed using an unfiltered 650 W light source directed at the sample placed in liquid nitrogen in a silvered dewar. 5 min illumination under these conditions produced maximum photoreduction of Q_A.

EPR spectrometry was performed at cryogenic temperatures using a JEOL RE1X spectrometer fitted with an Oxford Instruments liquid helium cryostat. Spectra were recorded and manipulated using a Dell microcomputer running ASYST software. Characteristic lineshapes were established by examining several sets of samples involving separate batches of PS II preparations. EPR conditions for the spectra shown were: microwave power, 10 mW, temperature, 4.4 K and modulation width, 1.25 mT.

Results

Higher plant PS II was investigated to determine whether the $g = 1.66$ EPR signal from Q_A^--Fe^{2+}-Q_B^- found in cyanobacteria [20] could be detected. Fig. 1 compares iron-semiquinone EPR signals in pea PS II either frozen to 77 K under illumination (Fig. 1a) or

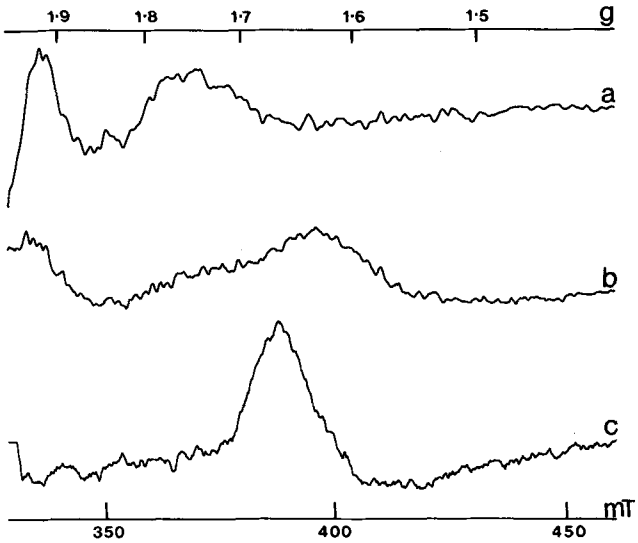

Fig. 1. Iron-semiquinone EPR spectra of pea PS II and *P. laminosum* PS II. (a) The spectrum of Q_A. The sample was frozen under illumination and stored in the dark for 1 week at 77 K, and then Q_A was photoreduced by 77 K illumination. (b) and (c) Spectra induced by 77 K illumination of samples frozen in the dark after treatment by the Q_B semiquinone protocol. Pea PS II sample (b) and *P. laminosum* PS II (c). Other conditions as in Materials and Methods.

illuminated at 77 K following a 45 min period of dark adaptation after illumination at 0°C (Fig. 1b). The lineshape differences are clear with the spectrum in Fig. 1b having a peak at $g = 1.63$ which can be compared with the spectrum of Q_A^--Fe^{2+}-Q_B^- obtained by illumination of *Phormidium laminosum* PS II at 77 K (Fig. 1c). As Fig. 1a shows, the illumination during freezing ensures the double reduction of Q_B, whilst the protocol used to obtain the spectra in Fig. 1b and 1c maximises the Q_B semiquinone levels before freezing [20].

The $g = 1.63$ peak in Fig. 1b is observed only below 20 K, increasing in size as the temperature is lowered. Detection of the peak also requires high microwave powers, suggesting the involvement of a transition metal consistent with the assignment to Q_A^--Fe^{2+}-Q_B^-. The mixture of $g = 1.9$ and $g = 1.6$ forms detected in Fig. 1b suggests that Q_B semiquinone cannot be generated in all centres as in the cyanobacterial PS II. This may be due to decay of some of the Q_B semiquinone formed by the illumination at room temperature or to a restricted pool of plastoquinone in the isolated PS II. The shift in *g*-value compared to the cyanobacterial signal could be caused by a variety of factors, including the isolation procedure or slight differences in structure of the quinone binding pockets.

The detection of EPR signals from iron-semiquinones in untreated thylakoid membranes is difficult. This is due to the presence in the spectrum of stronger signals from PS I iron-sulphur centres, which are also photo-reduced by 77 K illumination. However Fig. 2 shows that the higher field location and characteristic EPR conditions allow the $g = 1.63$ signal to be observed in thylakoid membranes. In Fig. 2a a sample subjected to the Q_B semiquinone protocol displays a $g = 1.9$ spectrum in the dark which can be attributed to Q_B^--Fe^{2+}. The $g = 1.9$ form of the signal indicates that it is from centres where bicarbonate is bound [14,21–22]. Following 77 K illumination to photoreduce Q_A (Fig. 2b), changes in the $g = 1.9$ region are obscured by reduction of iron-sulphur centre A of Photosystem I (arrowed) but the production of a broad signal near $g = 1.63$, attributed to Q_A^--Fe^{2+}-Q_B^-, is observed. The signal was also observed in chloroplast membranes from the barley mutant zb^{63} (Fig. 2c) which lacks photosystem 1. Fig. 2d shows the spectrum obtained from isolated Triton X-100-prepared PS II for comparison. The peak near $g = 1.6$ is therefore a characteristic of native PS II and is not a result of changes induced by preparative procedures.

Further confirmation of the identity of the signal near $g = 1.6$ was provided by the addition of PS II herbicide inhibitors or exogenous electron acceptors prior to the Q_B semiquinone protocol and 77 K illumination. Fig. 3a shows the untreated PS II sample exhibiting both $g = 1.9$ and $g = 1.6$ signals. Fig. 3b

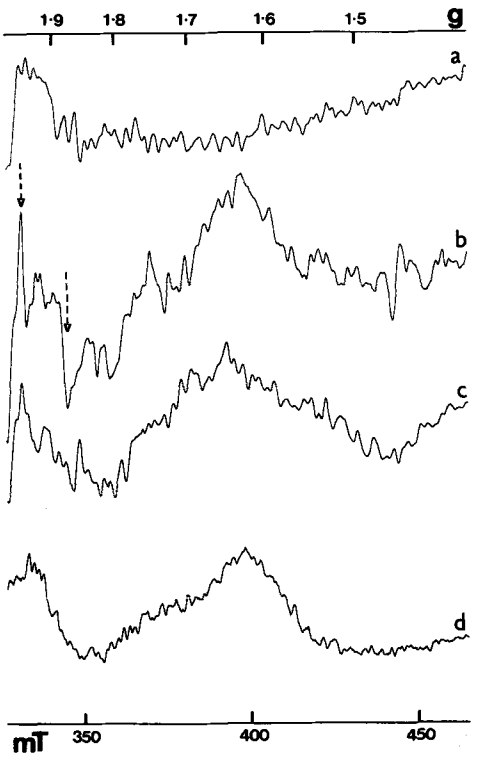

Fig. 2. Iron-semiquinone EPR spectra of thylakoid membranes (a–c) and pea PS II. (a) Pea thylakoid membranes frozen in the dark. (b) 77 K illuminated minus dark spectrum of sample in (a). (c) 77 K illuminated minus dark spectrum of barley zb^{63} mutant thylakoid membranes. (d) 77 K illuminated minus dark spectrum of pea PS II. The EPR signals from iron-sulphur centre A of PS I in (b) are arrowed. Other conditions as in Materials and Methods.

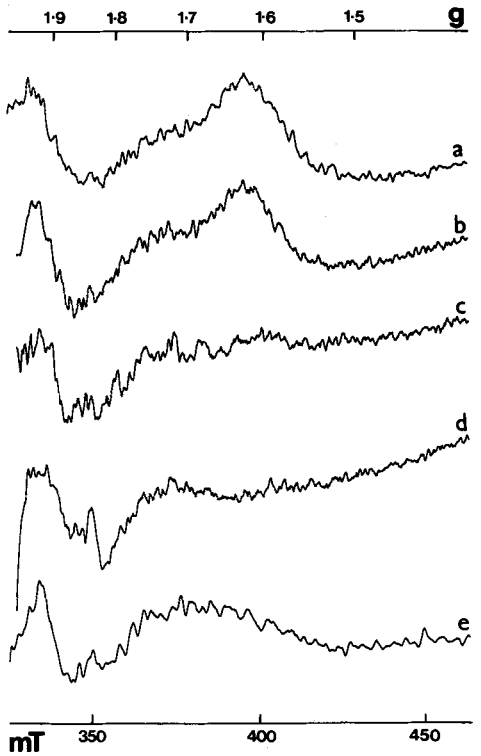

Fig. 3. Iron-semiquinone EPR difference spectra of pea PS II samples. 77 K illuminated minus dark spectra of samples prepared using the Q_B semiquinone protocol. (a) No additions or treated with (b) DCBQ (c) PPBQ (d) DCMU and (e) OP. Other conditions as in Materials and Methods.

shows the sample containing the Q_B analogue DCBQ , an electron acceptor known to have a relatively stable semiquinone and a limited ability to oxidise the non-haem iron [5,6,33,34]. Only a slight change in the lineshape and size of the signal occurs. Fig. 3c shows that when PPBQ, an electron acceptor with a semiquinone capable of oxidising the non-haem iron [5,6], is used, the $g = 1.6$ signal is removed and the $g = 1.9$ lineshape is sharpened and its amplitude is decreased.

Addition of the inhibitors DCMU (Fig. 3d) and *o*-phenanthroline (OP, Fig. 3e), which act by competing for the Q_B binding site, results in the absence of the the $g = 1.6$ signal. DCMU produces a characteristic mixture of $g = 1.9$ and $g = 1.8$ Q_A^--Fe^{2+} signals at this pH, suggesting that two types of binding occur, one of which causes displacement of bicarbonate from the non-haem iron. OP produces a $g = 1.9$ signal with a broadened trough near $g = 1.7$ as noted previously [35].

In order to remove the effects of Q_B redox changes from experiments on the charge accumulation process of the water oxidation system, Lavergne [36] used FCCP to cause rapid decay of the higher S states, S2 and S3. This prevented the decay of Q_B^- which would have undergone backreaction with S2 or S3 in untreated samples. Fig. 4 shows that use of FCCP to increase the yield of Q_B^- also increases the yield of the $g = 1.63$ signal (Fig. 4b).

The above results assign the $g = 1.6$ signal to Q_A^--Fe^{2+}-Q_B^-. It is also apparent that the ability to generate the signal is decreased in PS II compared to thylakoid or cyanobacterial membranes. It has been suggested previously that PS II prepared with Triton X-100 is depleted in plastoquinone [6]. Therefore, a quinone which would act as an artificial Q_B was sought in order to increase the yield of the $g = 1.6$ signal. Some quinones such as PPBQ are eliminated due to their ability to oxidise the non-haem iron through the Q_B site in their semiquinone form [5,6]. However, halogenated 1,4-benzoquinones have relatively stable semiquinones [34] and, as indicated by DCBQ in Fig. 3, allow the observation of the $g = 1.6$ signal. Tribromotoluquinone, TBTQ, was used to form a modified $g = 1.6$ signal in Ref. 20. We tested a number of quinones and found the brominated quinones DBMIB, bromanil and in particular TBTQ to be useful as Q_B substitutes for further experiments.

Fig. 5 (left) shows the dark EPR spectra of samples containing the brominated quinones which were treated using the Q_B semiquinone protocol. Fig. 5a shows the $g = 1.9$ signal from Q_B^--Fe^{2+} in an untreated PS II sample. When DBMIB is present a trough in the $g = 1.9$ region was observed (Fig. 5b), whilst in the presence of TBTQ (Fig. 5c) or bromanil (Fig. 5d) a

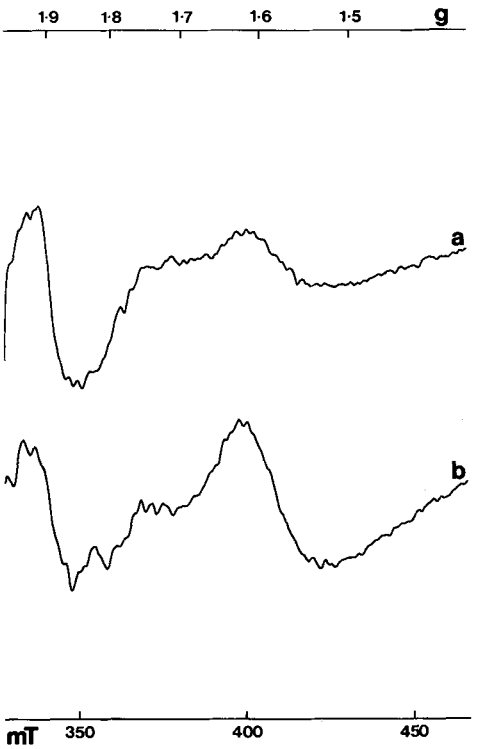

Fig. 4. EPR spectra showing the increased $g = 1.63$ peak (Q_A^--Fe^{2+}-Q_B^-) in FCCP treated samples. 77 K illuminated spectra of Q_B semiquinone protocol prepared samples. (a) No additions; (b) FCCP-treated. Other conditions as in Materials and Methods.

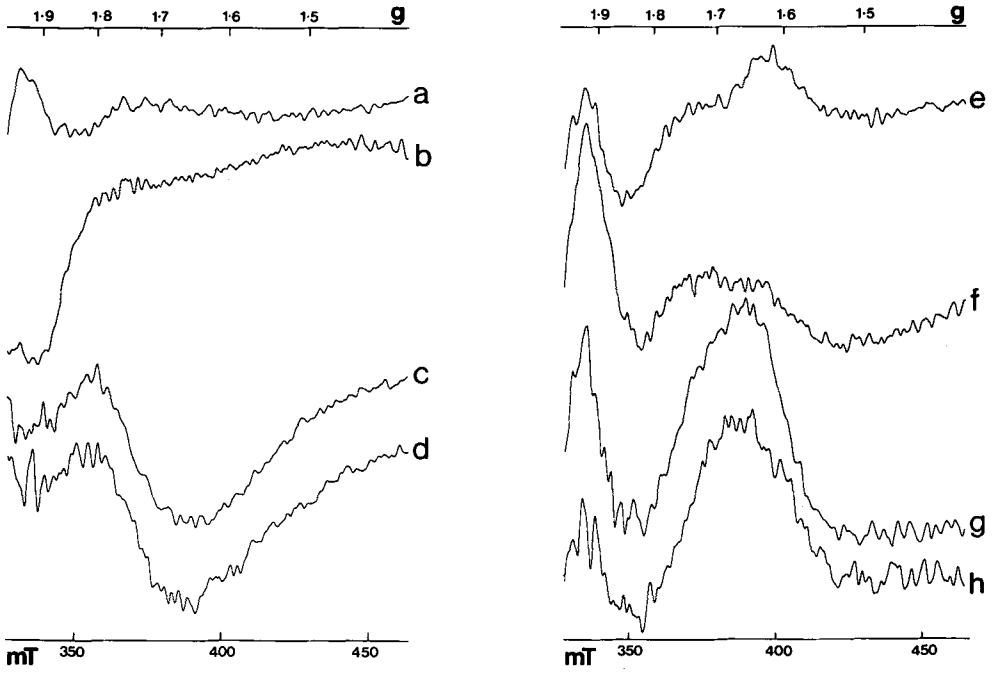

Fig. 5. Iron-semiquinone EPR spectra of brominated quinone-treated samples prepared using the Q_B semiquinone protocol. Dark (left) and 77 K illuminated minus dark (right) difference spectra. (a, e) no additions and treated with (b, f) DBMIB (c, g) TBTQ and (d, h) bromanil. Other conditions as in Materials and Methods.

broad $g = 1.8$-type signal with a trough centered in the $g = 1.6$ to $g = 1.7$ region was observed. The characteristics of this signal are described elsewhere [19] but the temperature, lineshape and microwave power saturation properties are consistent with its arising from a semiquinone interacting with the non-haem iron. Fig. 5 (right) shows the 77 K illuminated-minus-dark difference spectra. Following 77 K illumination, peaks between $g = 1.6$ and $g = 1.7$ (Q_A^--Fe^{2+}-Q_B^-) are generated in the untreated, TBTQ and bromanil samples consistent with the presence of Q_B^--Fe^{2+}in the dark. The peaks near $g = 1.6$ are broader and shifted to higher g-values compared with the native signal.

The DBMIB sample (Fig. 5b) has a $g = 1.9$ signal following illumination, suggesting that the interaction between Q_A and Q_B semiquinones is absent. The increased amplitude of the $g = 1.9$ signal results from illumination at 77 K both removing the trough seen in the dark (possibly $DBMIB^-$-Fe^{2+}) and inducing a $g = 1.9$ signal (Q_A^--Fe^{2+}).

The binding of the brominated quinones was also studied using the EPR signal from the oxidised non-haem iron [5,6]. Exogenous quinones bound to the Q_B site have been shown to affect this signal [37], causing changes in the lineshape and splitting of the major peaks near $g = 6$. Fig. 6 shows the EPR spectrum of the photoreduced non-haem iron in PS II samples oxidised by ferricyanide. The spectra were obtained by subtraction of the 77 K illuminated spectrum from the dark spectrum. The oxidised non-haem iron acts as an electron acceptor and is photoreduced at this temperature. In oxidised PS II (Fig. 6a), the characteristic peaks at $g = 8.1$ and $g = 1.6$ are seen. In the DBMIB sample (Fig. 6b), the oxidation of the non-haem iron is decreased, whilst in the TBTQ (Fig. 6c) and bromanil

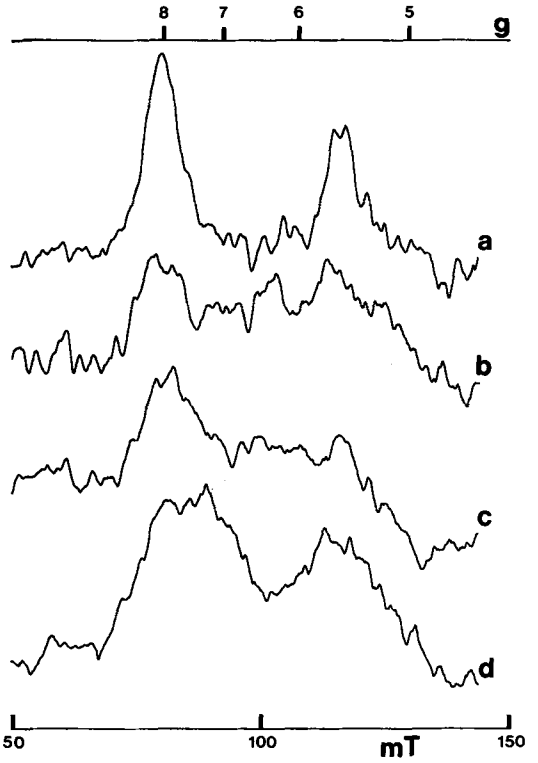

Fig. 6. EPR spectra of the ferricyanide oxidised non-haem iron. Dark minus 77 K illuminated (Fe^{3+} photoreduced) difference spectra of samples at pH 7.5. (a) No additions or treated with (b) DBMIB (c) TBTQ or (d) bromanil prior to ferricyanide treatment. Other conditions as in Materials and Methods.

samples (Fig. 6d) there are also lineshape and g-value changes. These are all indicative of the binding of these quinones in the Q_B pocket.

Although larger $g = 1.6$ EPR signals were obtained if the Q_B semiquinone protocol was followed after addition of TBTQ, the yield of Q_B^--Fe^{2+} obtained from samples dark adapted for 4 h without prior illumination was also greatly increased in the presence of TBTQ. This suggested that TBTQ semiquinone was relatively stable and was present in the stock solution or generated by interaction with PS II components such as native Q_B^- in the dark. Examination of stock solutions revealed that DCBQ, DBMIB, TBTQ and bromanil all gave EPR signals near $g = 2$ from the respective anionic semiquinones (not shown).

Renger and co-workers [24–26] suggested that one mode of action of TBTQ was possibly through covalent binding in the Q_B pocket. Fig. 7 shows that we have investigated this using competition with DCMU. Fig. 7a shows the spectrum in the dark of a TBTQ-containing sample treated by the Q_B semiquinone protocol and which has the signal attributed to $TBTQ_B^-$-Fe^{2+}. This signal is decreased if DCMU is added after illumination of a TBTQ sample at room temperature (Fig. 7b) and completely removed if DCMU is added before the period of illumination (Fig. 7c). 77 K illumination of samples a–c then produces EPR spectra which contain $g = 1.65$ signal in the TBTQ sample a (Fig. 7d), a trace of $g = 1.65$ signal in sample b (Fig. 7e) and no $g = 1.65$ signal in sample c (Fig. 7f). This shows that DCMU is able to displace TBTQ and suggests that it is more difficult to displace TBTQ in the semiquinone form, $TBTQ_B^-$. The data confirm the relationship of the dark (Q_B^--Fe^{2+}) and 77 K illuminated (Q_B^--Fe^{2+}-Q_A^-) signals and shows that covalent binding of TBTQ does not occur under our experimental conditions.

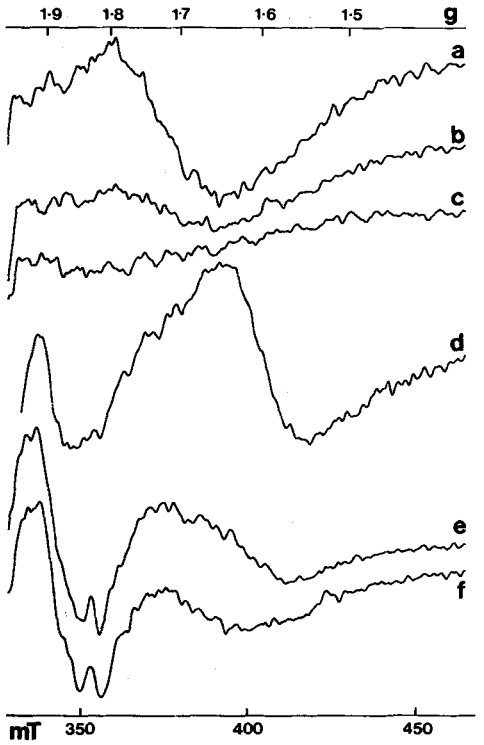

Fig. 7. EPR spectra showing competition between TBTQ and DCMU for the Q_B binding site. Spectra a–c are spectra before and d–f are spectra following 77 K illumination. Samples (a) and (d) are TBTQ-treated and prepared using the Q_B semiquinone protocol. Samples (b) and (e) are TBTQ-treated, illuminated at room temperature as in the Q_B semiquinone protocol and then DCMU-treated before freezing to 77 K in the dark. Samples (c) and (f) are TBTQ-treated and DCMU is added before the illumination step of the Q_B protocol. Other conditions as in Materials and Methods.

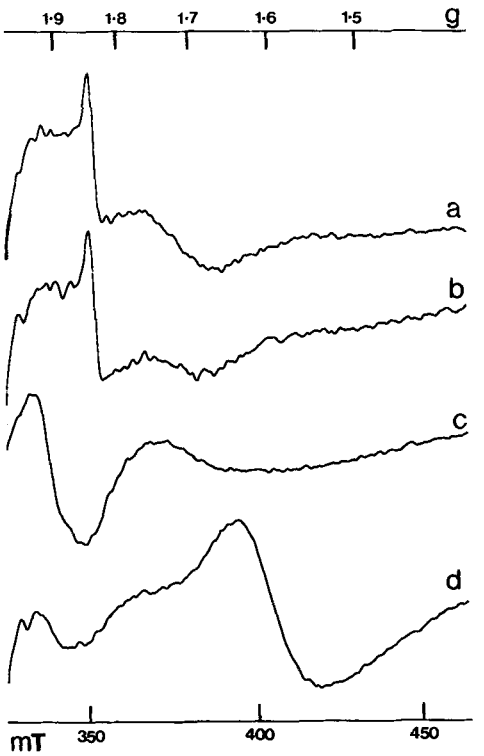

Fig. 8. EPR spectra showing the bicarbonate requirement for the interaction between Q_A and Q_B. Spectra shown are HTG PS II after 77 K illumination. (a) and (b) HTG PS II at pH 6.0 and (c) and (d) at pH 7.5. Samples (a) and (c) had no additions whilst (b) and (d) were TBTQ treated. Other conditions as in Materials and Methods.

PS II preparations which lack native Q_B and which can either retain or lack bound bicarbonate have recently been developed [29] using the detergent HTG. These were used to determine whether bicarbonate binding was required in order to detect the $g = 1.6$ signal. Fig. 8 shows that in the absence of bicarbonate in HTG PS II samples at pH 6 a peak at $g = 1.84$ (Fig. 8a) is obtained upon 77 K illumination which is only slightly altered by the presence of TBTQ (Fig. 8b). Untreated HTG PS II samples at pH 7.5 which retain bicarbonate give a $g = 1.9$ signal from Q_A^--Fe^{2+} following 77 K illumination (Fig. 8c) but samples containing TBTQ give the $g = 1.6$ signal from Q_B^--Fe^{2+}-Q_A^- (Fig. 8d). This result shows that bound bicarbonate is re-

quired to observe the interaction between the semiquinones producing the $g = 1.6$ signal.

Discussion

We have shown that two sources of heterogeneity in PS II preparations, bicarbonate bound or absent and Q_B bound or absent can now be monitored by EPR.

We have demonstrated that the interaction discovered in cyanobacteria [12,13,20] between the semiquinones of Q_A and Q_B also occurs in higher plant PS II. An important observation is that bicarbonate binding to PS II is required for this interaction. McDermott et al. [12] speculated that differences between cyanobacteria and higher plants in the amino-acid sequence, and therefore in the structure of the quinone binding loops, resulted in a cyanobacterial $g = 1.6$ signal from Q_A^--Fe^{2+}. We have shown that this is not so [20], but structural differences may account for the g-value differences between the interaction of Q_A and Q_B semiquinones in cyanobacteria and plants.

The alteration of the EPR characteristics of the iron semiquinones in PS II by bicarbonate binding could explain the absence of the signal in photosynthetic bacteria. The interaction of the two semiquinones in photosynthetic bacteria reduces the size of the iron semiquinone signals [38] and can be explained as an exchange interaction resulting in spin states with integer total spin. These can be EPR-silent or give altered EPR spectra. Clearly the interaction in PS II is different, which may be a result of the bound bicarbonate or may involve a third paramagnetic species. The only PS II species always present in our experiments when the $g = 1.6$ signal was formed was oxidised cytochrome b-559. Further experiments will investigate the possible influence of this centre. The physical parameters which may give rise to the lineshapes of the iron-semiquinone signals are discussed further in Ref. 19.

Rutherford et al. [21] showed that a change in $g = 1.9$ lineshape occurred under conditions where Q_A^- to Q_B electron transfer was possible and attributed this to Q_B^--Fe^{2+}. In this paper and previously [22] we have also shown that Q_B^--Fe^{2+} can have a $g = 1.9$ lineshape similar to that of Q_A^--Fe^{2+}. However, we also show that changes in the $g = 1.9$ lineshape occur as a result of addition of herbicides or the interaction of the Q_A and Q_B semiquinones (Figs. 3–5). The most appropriate marker for Q_B^--Fe^{2+} is therefore the appearance of the $g = 1.6$ signal following 77 K illumination.

DBMIB was introduced as an inhibitor of photosynthetic electron transport 20 years ago [39]. Further work has shown that halogen-substituted 1,4-benzoquinones can inhibit at Photosystem II and the cytochrome b/f complex [23]. A direct interaction between certain halogen substituted 1,4-benzoquinones (e.g., DBMIB) and the Rieske iron-sulphur protein of the cytochrome b/f complex has been demonstrated by EPR [40]. We have now demonstrated that brominated quinones, especially TBTQ and bromanil, can be used as a substitute Q_B in PS II to study Q_B behaviour.

Previous studies on brominated 1,4-benzoquinones have suggested tight (possibly covalent) binding to PS II. However, covalent binding was not a prerequisite for inhibition, as this occurred immediately, whilst covalent attachment was time-dependent [24–26]. Studies showed that, when added before DCMU, these quinones were able to accept electrons from Q_A^- in a DCMU-insensitive reaction. However preincubation with DCMU prevented binding. The conclusion was that either TBTQ bound tightly at the Q_B site and was modified by allosteric effects on DCMU binding or that a DCMU–TBTQ exchange occurred which is fast in the light and slow in the dark [26]. Our experiments show that the latter mechanism operates as TBTQ is bound as the semiquinone in the dark. In Refs. 24 and 26 this allowed a single turnover of the PS II reaction centre to give the quinol, which could then be displaced more easily by DCMU.

The affinity of Q_B for its binding site is known to be much higher in the semiquinone form [3,4]. The effect of the tight binding and stability of the TBTQ semiquinone is to lower its redox potential [3,4,34]. This explains the absence of oxidation of the non-haem iron by TBTQ semiquinone, as this has been shown to depend on the redox potential of the Q_B^-/Q_BH_2 couple. Oxidation of the non-haem iron by ferricyanide is also slowed, as the quinone in the Q_B site reduces accessibility of ferricyanide to the iron.

The characteristics of the $TBTQ_B^-$-Fe^{2+} signal are similar to the $g = 1.8$ type bicarbonate-free Q_A^--Fe^{2+} signals. However, following illumination to reduce Q_A, the $g = 1.9$ and $g = 1.6$ signals are still observed, indicating that bicarbonate is still bound. Blubaugh and Govindjee [15] have proposed two sites of bicarbonate binding: (1) a binding to the non-haem iron and D2 in a structural role and (2) a binding to an arginine on D1 and a role in protonation. If TBTQ displaces bicarbonate from only the D1 Q_B site this would account for the EPR characteristics of the iron-semiquinone , oxidised non-haem iron and the inhibition of electron transfer as protonation of Q_B would be impaired.

Further experiments will investigate these aspects as well as the protonation events at the Q_B site.

Acknowledgements

This work was supported by the U.K. Science and Engineering Research Council. We would like to thank Professor W. Oettmeier for his gift of TBTQ, Dr P. Rich for his gift of bromanil and Dr David Simpson for seed of barley mutant zb^{63}. We also thank Professor

M.C.W. Evans and Drs. Gang Li, Dugald Maclachlan and Andrew Corrie for helpful discussion.

References

1 Michel, H. and Deisenhofer, J. (1988) Biochemistry 27, 1–7.
2 Feher, G., Allen, J.P., Okamura, M.Y. and Rees, D.C. (1989) Nature 339, 111–116.
3 Crofts, A.R. and Wraight, C.A. (1983) Biochim. Biophys. Acta 726, 149–185.
4 Wraight, C.A. (1981) Isr. J. Chem. 21, 348–354.
5 Zimmermann, J.L. and Rutherford, A.W. (1986) Biochim. Biophys. Acta 851, 416–423.
6 Diner, B.A. and Petrouleas, V. (1987) Biochim. Biophys. Acta 895, 107–125.
7 Trebst, A. (1987) Z. Naturforsch. 42c, 742–750.
8 Butler, W.F., Calvo, R., Fredkin, D.R., Isaacson, R.A., Okamura, M.Y. and Feher, G. (1984) Biophys. J. 45, 947–973.
9 Nugent, J.H.A., Diner, B. and Evans, M.C.W. (1981) FEBS Lett. 124, 241–244.
10 Evans, M.C.W., Diner, B.A. and Nugent, J.H.A. (1982) Biochim. Biophys. Acta 682, 97–105.
11 Rutherford, A.W. and Zimmermann, J.L. (1984) Biochim. Biophys. Acta 767, 168–175.
12 McDermott, A.E., Yachandra, V.K., Guiles, R.D., Cole, J.L., Dexheimer, S.L., Britt, R.D. Sauer, K. and Klein, M.P. (1988) Biochemistry 27, 4021–4031.
13 Nugent, J.H.A., Corrie, A.C., Demetriou, C., Evans, M.C.W. and Lockett, C.J. (1988) FEBS Lett. 235, 71–75.
14 Vermaas, W.F.J. and Rutherford, A.W. (1984) FEBS Lett. 175, 243–248.
15 Blubaugh, D. and Govindjee (1988) Photosynth. Res. 19, 85–128.
16 Van Rensen, J.J.S., Tonk, W.J.M. and Bruijn, S.M. (1988) FEBS Lett. 226, 347–351.
17 Diner, B.A. and Petrouleas, V. (1990) Biochim. Biophys. Acta 1015, 141–149.
18 Petrouleas, V. and Diner, B.A. (1990) Biochim. Biophys. Acta 1015, 131–140.
19 Reference deleted
20 Corrie, A.C. Nugent, J.H.A. and Evans, M.C.W. (1991) Biochim. Biophys. Acta 1057, 384–390.
21 Rutherford, A.W., Zimmerman, J.L., and Mathis, P. (1984) in Advances in Photosynthesis Research, Vol. 1, 445–448 (Sybesma, C., ed), Martinus Nijhoff/Dr W. Junk Publishers, Dordrecht.
22 Evans, M.C.W., Nugent, J.H.A., Hubbard, J.A.M., Demetriou, C., Lockett, C.J. and Corrie, A.R. (1988) in Plant Membranes – Structure, Assembly and Function (Harwood, J.L. and Walton, T.J., eds.), pp. 149–158, Biochemical Society, London.
23 Oettmeier, W., Masson, K. and Dostatni, R. (1987) Biochim. Biophys. Acta 890, 260–269.
24 Renger. G., Kayed, A. and Oettmeier (1987) Z. Naturforsch. 42c, 698–703.
25 Renger, G. Hanssum, B., Gleiter, H., Koike, H. and Inoue, Y. (1988) Biochim. Biophys. Acta 936, 435–446.
26 Renger, G. Messinger, J. and Fromme, R. (1989) Z. Naturforsch. 44c, 423–430.
27 Ford, R.C. and Evans, M.C.W. (1983) FEBS Lett. 160, 159–163.
28 Enami, I., Kamino, K., Shen, J.R., Satoh, K. and Katoh, S. (1989) Biochim. Biophys. Acta 977, 33–39.
29 Bowden, S.J., Hallahan, B.J., Ruffle, S.V., Evans, M.C.W. and Nugent, J.H.A. (1991) Biochim. Biophys. Acta 1060, in press.
30 Arnon, D.I. (1949) J. Plant Physiol. 24, 1–15.
31 Stewart, A.C. and Bendall, D.S. (1979) FEBS Lett. 107, 308–312.
32 Schatz, G.H. and Witt, H.T. (1984) Photochem. Photobiophys. 7, 1–14 and 77–89.
33 Hoganson, C.W. and Babcock, G.T. (1988) Biochemistry 27, 5848–5855.
34 Rich, P.R. and Bendall, D.S. (1980) Biochim. Biophys. Acta 592, 506–518.
35 Rutherford, A.W., Zimmermann, J.L. and Mathis, P. (1984) FEBS Lett. 165, 156–162.
36 Lavergne, J. (1987) Biochim.Biophys. Acta 894, 91–107.
37 Diner, B.A. and Petrouleas, V. (1987) Biochim. Biophys. Acta 893, 138–148.
38 Wraight, C.A. (1978) FEBS Lett. 93, 283–288.
39 Trebst, A., Harth, E. and Draber, W. (1970) Z. Naturforsch. 2Sb 1157–1159.
40 Malkin, R. (1981) FEBS Lett. 131, 169–172.